SOLAR/2041-79/14
Distribution Category UC-59

SOLAR-ENERGY-SYSTEM PERFORMANCE EVALUATION

NORTHVIEW ELEMENTARY SCHOOL
(HOWARD'S GROVE)
HOWARD'S GROVE, WISCONSIN

SEPTEMBER 1978 THROUGH APRIL 1979

KENNETH L. SHENFISH, PRINCIPAL AUTHOR
W. H. McCUMBER, MANAGER OF PERFORMANCE ANALYSIS
LARRY J. MURPHY, IBM PROGRAM MANAGER

IBM CORPORATION
150 SPARKMAN DRIVE
HUNTSVILLE, ALABAMA 35805

PREPARED FOR THE
DEPARTMENT OF ENERGY
OFFICE OF ASSISTANT
SECRETARY FOR
CONSERVATION AND SOLAR APPLICATIONS
UNDER CONTRACT EG-77-C-01-4049
H. JACKSON HALE, PROGRAM MANAGER

TABLE OF CONTENTS

LIST OF FIGURES AND TABLES

NATIONAL SOLAR DATA PROGRAM REPORTS

Reports prepared for the National Solar Data Program are numbered under a specific format. For example, this report for Northview Elementary School (Howard's Grove) project site is designated as SOLAR/2041-79/14. The elements of this designation are explained in the following illustration.

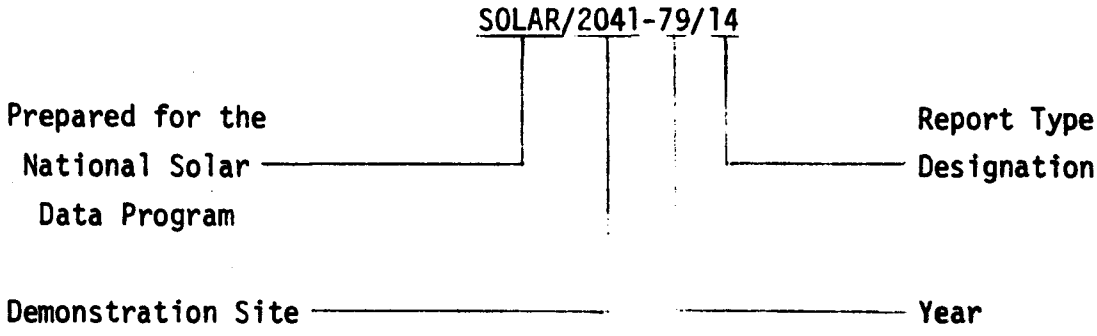

- Demonstration Site Number:

  Each Project site has its own discrete number - 1000 through 1999 for residential sites and 2000 through 2999 for commercial sites.

- Report Type Designation:

  This number identifies the type of report, e.g.,

  - Monthly Performance Reports are designated by the numbers 01 (for January) through 12 (for December).

  - Solar Energy System Performance Evaluations are designated by the number 14.

  - Solar Project Descriptions are designated by the number 50.

  - Solar Project Cost Reports are designated by the number 60.

These reports are disseminated through the U. S. Department of Energy, Technical Information Center, P. O. Box 62, Oak Ridge, Tennessee 37830.

1. FOREWORD

The National Program for Solar Heating and Cooling is being conducted by the Department of Energy under the Solar Heating and Cooling Demonstration Act of 1974. The overall goal of this activity is to accelerate the establishment of a viable solar energy industry and to stimulate its growth in order to achieve a substantial reduction in non-renewable energy resource consumption through widespread applications of solar heating and cooling technology.

Information gathered through the Demonstration Program is disseminated in a series of site-specific reports. These reports are issued as appropriate and may include such topics as:

- Solar Project Description
- Design/Construction Report
- Project Costs
- Maintenance and Reliability
- Operational Experience
- Monthly Performance
- System Performance Evaluation

The International Business Machines Corporation is contributing to the overall goal of the Demonstration Act by monitoring, analyzing, and reporting the thermal performance of solar energy systems through analysis of measurements obtained by the National Solar Data Program.

The System Performance Evaluation Report is a product of the National Solar Data Program. Reports are issued periodically to document the results of analysis of specific solar energy system operational performance. This report includes system description, operational characteristics and capabilities, and an evaluation of actual versus expected performance. The Monthly Performance Report, which is the basis for the System Performance Evaluation Report, is published on a regular basis. Each parameter

presented in these reports as characteristic of system performance represents over 8,000 discrete measurements obtained each month by the National Solar Data Network.

All reports issued by the National Solar Data Program for the Northview Elementary School (Howard's Grove), solar energy system are listed in Section 6, References.

This Solar Energy System Performance Evaluation Report presents the results of a thermal performance analysis of the Northview Elementary School (Howard's Grove) solar energy system. The analysis covers operation of the system from September 1978 through April 1979. The Northview Elementary School (Howard's Grove) solar energy system provides space heating to an Elementary School located in Howard's Grove, Wisconsin. A more detailed system description is contained in Section 3. Analysis of the system thermal performance was accomplished using a system energy balance technique described in Section 4. Section 2 presents a summary of the results and conclusions obtained while Section 5 presents a detailed assessment of the system thermal performance.

Acknowledgements are extended to those individuals involved in the operation of the Northview Elementary School (Howard's Grove) solar energy system. Their insight and cooperation in the resolution of various on-site problems during the reporting period were invaluable.

2. SUMMARY AND CONCLUSIONS

This System Performance Evaluation report provides an operational summary of the solar energy system installed at the Northview Elementary School (Howard's Grove) located at Howard's Grove, Wisconsin. This analysis is conducted by evaluation of measured system performance and by comparison of measured weather data with long-term average climatic conditions. The performance of major subsystems is also presented.

The measurement data were collected [References 8-15]* by the National Solar Data Network (NSDN) [1] for the period September 1978 through April 1979. System performance data are provided through the NSDN via an IBM-developed Central Data Processing System (CDPS) [2]. The CDPS supports the collection and analysis of solar data acquired from instrumented systems located throughout the country. This data is processed daily and summarized into monthly performance reports. These monthly reports form a common basis for system evaluation and are the source of the performance data used in this report.

Features of this report include: a system description, a review of actual system performance during the report period, analysis of performance based on evaluation of meteorological load and operational conditions, and an overall discussion of results.

The Northview Elementary School addition (Howard's Grove) solar energy site was installed and checked out on August 25, 1978. The data communications system was brought on-line September 7, 1978 and solar system operation began on September 29, 1978 with the onset of the space heating season.

On October 25, 1978 two sensor problems were resolved. The outside ambient temperature sensor range was increased to enable measurement of the extremely low temperatures that can occur at this locality and the sensor that measures the controlled infiltration rate of outside air was rescaled to a more appropriate range.

---

*Numbers in brackets designate References found in Section 6.

A communication system power transient is believed to be responsible for disabling several measurements on November 15, 1978. The system was repaired on November 30, 1978. Several lost measurements were estimated by using data for the first part of November and measured system hardware performance.

In early November a half-closed fire damper door was discovered. Prior to this time, the collector flow was reduced by a factor of two which resulted in poor collector subsystem performance. The condition was alleviated by opening the door on November 8.

On December 1, the fuel oil burner power measurement technique was modified to permit a more accurate indication of burner fuel oil consumption.

Energy flow imbalances existing in the performance factor computations were alleviated in December, when it was found from analysis that the large, 7.5 HP circulating fan was adding significant energy to the building supply duct. This energy was properly accounted for and an energy flow balance for the solar system was achieved. Monthly reports for December and subquent months provide an accurate indication of solar system performance.

In January, large amounts of snow (30 inches) were deposited on the collectors. The collectors were entirely covered on some days in January. At the end of January, the lower third of the collectors was still covered, and this prevented normal operation of the system. The local solar system designer noticed this situation and advised maintenance personnel at the school to remove the snow. This was accomplished in late January. The low solar energy contribution that month is directly attributable to this condition.

In February, the performance of the solar energy system was significantly improved over earlier winter months. The major reason for the solar energy system performance improvement was an increase in collector array efficiency.

The improved collector array performance is believed to be due to higher collector leakage flow and temperatures and the normal movement of the operating point to lower values with a resulting increase in collector efficiency.

Leaky collectors act like a fresh air preheater that supplies fresh air to the building. The introduction of air through leaks along the collector array actually increases collector efficiency (Reference [7]).

The collector array efficiency in an air system normally improves as the collector array operating point shifts toward lower values experienced in spring months. As the ambient temperature rises and the collector inlet temperature remains essentially constant, the operating point shifts toward lower values and the collector array efficiency rises.

Monthly values of average daily insolation and average outdoor ambient temperature measured at the Northview Elementary School (Howard's Grove) site are presented in Table 5.1-1. Also presented in the table are the long-term, average monthly values for these climatic parameters.

Temperatures during the eight-month reporting period were slightly lower than normal with a measured average outdoor ambient temperature of 33°F as opposed to the long-term average of 35°F. During January and February, the measured outside ambient temperature was an average of 7°F lower than the long-term average for those months. This resulted in a greater number of measured heating degree-days (7,960 versus 7,275). The cooling degree-days were above normal because September was warmer than the long-term average. The average daily insolation measured (at a 50-degree tilt) was 1,123 Btu/ft^2 which is one percent less than the long-term daily average of 1,130 Btu/ft^2 for the months in the reporting period.

Both the long-term average temperature and insolation values were computed from averages derived from Milwaukee and Green Bay weather stations. Howard's Grove is about half-way between these weather stations.

During this reporting period, the system achieved a net space heating energy savings of 99.69 million Btu which is the equivalent of 691 gallons of fuel oil (based on a heating value of 144,400 Btu per gallon of fuel oil). A total of 30.05 million Btu of electrical energy was required to operate the system.

A total of 663.69 million Btu of incident solar energy was measured in the plane of the collector array during the reporting period. At times when the collector array was operating, there were 428.90 million Btu incident on the array. The system collected 101.03 million Btu, which represents an operational collector array efficiency of 24 percent. The collector array analysis revealed that the performance of the collector array was degraded during the harsh winter months due to the manner in which the collectors were operated. A significant collector array thermal lag exists during collector array turn-on. This is due to the collector thermal mass and large collector array losses associated with these collectors. Up to one-seventh of the solar energy available is not collected because of these conditions. The collector turn-on conditions should be adjusted to alleviate this condition in winter months.

A total of 98.16 million Btu was delivered to storage during the reporting period, and 76.59 million Btu were removed from storage for support of the space heating load. Although most of the energy delivered to storage was utilized to meet the space heating demand, the average storage temperature remained very close to the building temperature. Indeed, there were times when environmental energy from the building and outside infiltrations added energy to the rock bed and this energy was subsequently used to meet the space heating demand. Part of the reason for the stability of the rock bed average temperature was the energy contribution from the building air circulation fan. The circulation fan blade is very large (40 inches in diameter) and its rotation both warms the air and imparts the circulating velocity. The warm air causes the inlet temperature of the rock bed to be approximately 1.5 degrees higher than the building return temperature. This effect tends to stabilize the rock bed temperatures.

The average storage heat loss coefficient was 69 Btu/hr for the reporting period. However, there was a significant amount of scatter in the individual monthly values used to compute the average. The exact cause of the scatter is unknown, but it is suspected to be due to energy imbalances associated with temperature measurement inaccuracies coupled with extremely high air flow rates (approximately 11,000 cfm). Temperature biases and fluctuations could account for the scatter, but the magnitude of these uncertainties is less than the uncertainty (0.25°F) associated with the calibrated temperature probes. Therefore, variations of this magnitude for the storage heat loss coefficient might be expected under these operating conditions.

Analysis of the storage subsystem revealed that storage performance may be degraded because of a steel plenum barrier that was installed in the rock storage bin at the time of construction. Collected energy is stored in the top of rock storage between the collector inlet and the building return vertical inlet shaft. However, when energy is removed from rock storage, the air flow path is from the bottom of the storage bin to the supply duct outlet. This path does not pass through the portion of the rock that is heated by the collectors. Thus, the rock bed outlet temperatures are lower than desired. This condition results in auxiliary consumption during morning hours in the spring months which would not occur if this situation did not exist.

The controlled (measured) space heating load for the reporting period was 468.84 million Btu. Controlled solar energy supplied 76.59 million Btu of this load and the remaining 393.06 million Btu were supplied by the fuel oil furnace. This resulted in a solar fraction of 16 percent and a savings of 99.69 million Btu of fossil or, equivalently, 691 gallons of fuel oil. However, the circulating fan added additional energy to the building and losses from the solar duct work and storage also contributed to the space heating load.

The calculation of the space heating load is complicated by measurement uncertainties. The calculation of the space heating load using different sets of sensor configurations has produced widely differing results. Analysis of this condition indicates that the magnitude of the total system air flow is questionable. An air flow magnitude about 40 percent less than indicated would provide a more consistent result. The heating load calculated using the liquid flow measurements implies a fuel oil furnace/heat exchanger system efficiency of 60 percent. However, personnel at the site indicate that the efficiency is approximately 76 percent. Also, consumption figures obtained from the school indicate that the efficiency is somewhat higher than indicated by the system measurements. Therefore, the space heating subsystem performance computations are based on an assumed efficiency of 76 percent.

In general, the Northview Elementary School solar energy system performance was degraded until February when larger amounts of solar energy became available, collector infiltration air temperatures moderated, and the collector array operating point shifted to higher values of collector array efficiency. The increased performance was due to the improved collector performance after January 1979.

3. SYSTEM DESCRIPTION

This solar energy heating system is designed to provide 58 percent of the space heating for an addition to the North View Elementary School in Howards Grove, Wisconsin. The addition contains 12,330 square feet of heated space. The collector array has a total of 138 collector panels arranged in six rows, each row containing 23 flat-plate air collector panels. The array panels, manufactured by Sun Stone Solar Energy Equipment, have a gross area of 2,685 square feet. The collectors face south at an angle of 50 degrees from the horizontal. Air is the medium used for transferring energy from the collector array to storage. Solar energy is stored in a 16- by 21- by 6-foot concrete block bin containing 1,500 cubic feet of crushed rock located below the equipment room. When solar energy is inadequate to provide space heating, auxiliary thermal energy is supplied from a 397,200 Btu/hr fuel oil boiler. The space heating control system modulates control dampers to mix outside air, return air and thermally heated air (solar and auxiliary) to maintain a building temperature of 67°F during the day and 55°F at night. A minimum of 10 percent fresh outside air is required by law to be mixed with return air.

This system, shown schematically in Figure 3-1, has three modes of operation.

Mode 1 - Collector-to-Storage: This mode is entered when the collector array outlet temperature exceeds the temperature at the bottom of rock thermal storage by at least 17°F. Air is drawn from the collector array, using the collector circulating fan F2, into the rock thermal storage and recirculated to the collectors. This mode continues until the collector outlet temperature no longer exceeds the temperature in the bottom of rock thermal storage by at least 4°F.

Mode 2 - Storage-to-Classrooms (Occupied): This mode is entered at the beginning of each school day as determined by a seven-day clock timer. Circulation fan F1 runs continuously to transfer energy from storage, to

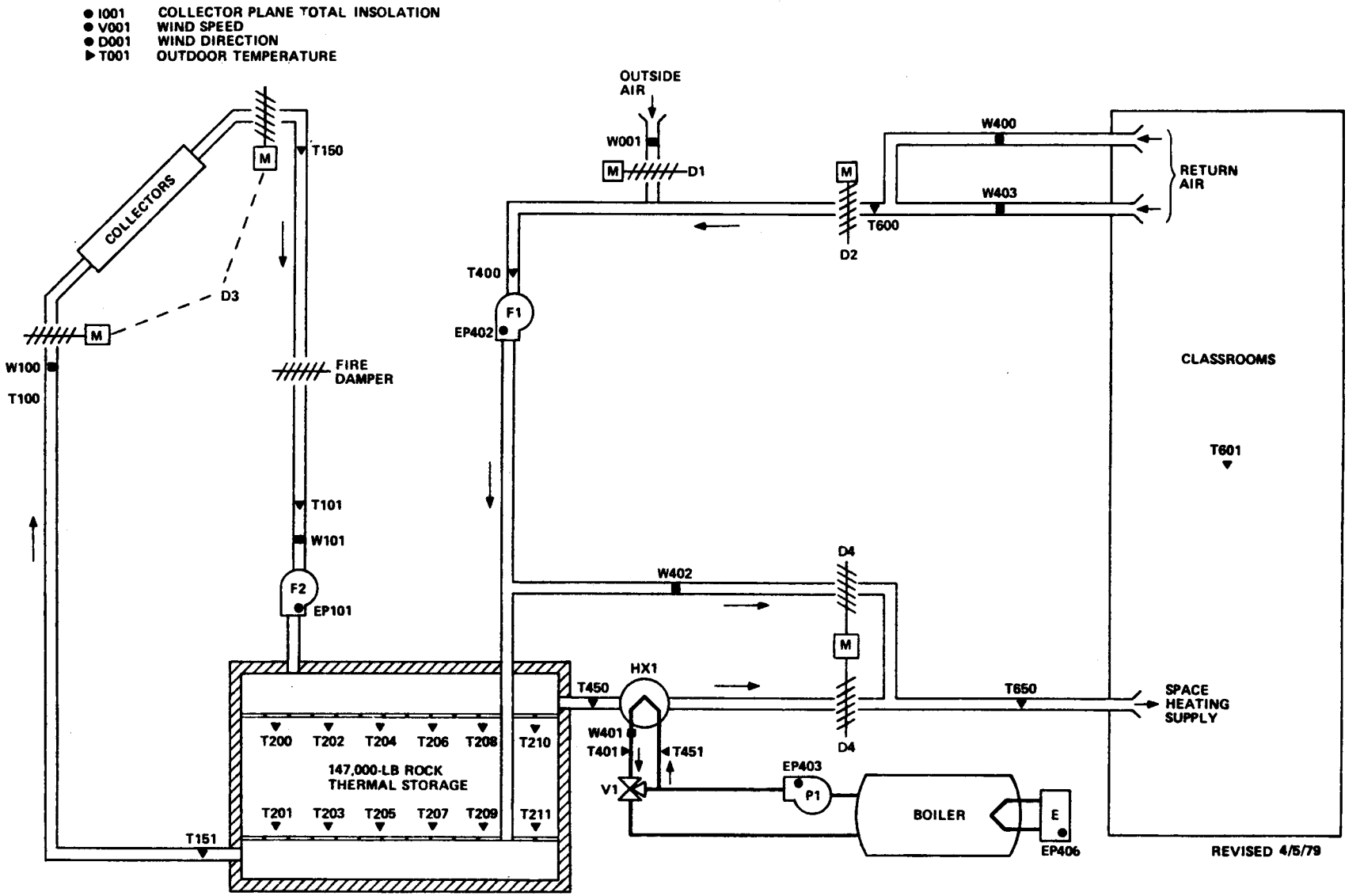

FIGURE 3-1 HOWARDS GROVE SCHOOL SOLAR ENERGY SYSTEM SCHEMATIC

classrooms, and to provide ventilation. Outside air and return air dampers are modulated to supply fresh air at a mixed return air temperature of 60°F. Multizone control dampers modulate the mixed return air with thermally heated air from storage to maintain the space heating system supply air temperature. The auxiliary fuel oil boiler supplements solar energy to meet the space heating demand, and to maintain the building's indoor ambient temperature. The seven-day clock timer terminates this mode at the end of each school day. The clock timer may be manually overridden to provide mode 2 heating for irregularly scheduled (outside normal class hours) school events.

Mode 3 - Storage-to-Classrooms (Unoccupied): This mode is entered when there is a demand for space heating and the system is not in the Occupied mode. The outside air damper D1 is closed. Circulating fan F1 runs when a space heating demand exists to transfer energy from storage to classrooms, and to provide ventilation. Multizone control dampers modulate the return air with thermally heated air from storage to maintain the space heating system supply temperature. The auxiliary fuel oil boiler supplements solar energy to meet the space heating demand and to maintain the building's indoor ambient temperatures. This mode terminates when either the demand for space heating ceases, or the system is changed to the Occupied mode.

Mode 1 operation can occur while either Mode 2 or Mode 3 is active.

4. PERFORMANCE EVALUATION TECHNIQUES

The performance of the Northview Elementary School (Howard's Grove) solar energy system is evaluated by calculating a set of primary performance factors which are based on those proposed in the intergovernmental agency report "Thermal Data Requirements and Performance Evaluation Procedures for the National Solar Heating and Cooling Demonstration Program" [3]. These performance factors quantify the thermal performance of the system by measuring the amount of energies that are being transferred between the components of the system. The performance of the system can then be evaluated based on the efficiency of the system in transferring these energies.

Data from monitoring instrumentation located at key points within the solar energy system are collected by the National Solar Data Network. This data is first formed into factors showing the hourly performance of each system component, either by summation or averaging techniques, as appropriate. The hourly factors then serve as a basis for the calculation of the daily and monthly performance of each component subsystem.

Each month a summary of overall performance of the Northview Elementary School (Howard's Grove) site and a detailed subsystem analysis are published. Monthly reports for the period covered by this System Performance Evaluation, September 1978 through April 1979, are available from the Technical Information Center, Oak Ridge, Tennessee 37830.

5. PERFORMANCE ASSESSMENT

The performance of the Northview Elementary School (Howard's Grove) solar energy system has been evaluated for the September 1978 through April 1979 time period. Two perspectives have been taken in this assessment. The first looks at the overall system view in which the total solar energy collected, the system load and the measured values for solar energy used and system solar fraction are presented. Also presented, where applicable, are the expected values for solar energy used and system solar fraction The expected values have been derived from a modified f-chart* analysis which uses measured weather and subsystem loads as inputs. The model used in the analysis is based on manufacturers' data and other known system parameters. In addition, the solar energy system coefficient of performance (COP) at both the system and subsystem level has been presented. The second view presents a more in-depth look at the performance of individual components. Details relating to the performance of the collector array and storage subsystems are presented first, followed by details pertaining to the space heating subsystem. Included in this area are all parameters pertinent to the operation of each individual subsystem.

The performance assessment of any solar energy system is highly dependent on the prevailing weather conditions at the site during the period of performance. The original design of the system is generally based on the long-term averages for available insolation and temperature. Deviations from these long-term averages can significantly affect the performance of the system. Therefore, before beginning the discussion of actual system performance, a presentation of the measured and long-term averages for critical weather parameters has been provided.

---

*f-chart is the designation of a procedure for designing solar heating systems. It was developed by the Solar Energy Laboratory, University of Wisconsin-Madison.

5.1 Weather Conditions

Average values of the daily incident solar energy in the plane of the collector array and the average outdoor temperature measured at the Northview Elementary School (Howard's Grove) site during the report period are presented in Table 5.1-1.

Also presented in Table 5.1-1 are the corresponding long-term average monthly values of the measured weather parameters. These data are taken from Reference Monthly Environmental Data for Systems in the National Solar Data Network [4]. A complete yearly listing of these values for the site is given in Appendix C.

Monthly values of heating and cooling degree-days are derived from daily values of ambient temperature. They are useful indications of the system heating and cooling loads. Heating degree-days and cooling degree-days are computed as the difference between daily average temperature and 65°F. For example, if a day's average temperature was 60°F, then five heating degree-days are accumulated. Likewise, if a day's average temperature was 80°F, then 15 cooling degree-days are accumulated. The total number of heating and cooling degree-days are summed monthly.

During the eight month period from September 1978 to April 1979, a daily average of 1,123 Btu/ft^2 of solar energy was incident on the collector array. This was one percent below the long-term daily average of 1,130 Btu/ft^2. The measured average ambient temperature for the period was 33°F, which was two degrees below the long-term average of 35°F.

Very cold temperatures experienced in January and February were responsible for an increased number of heating degree days (7,960 versus 7,275) during the reporting period. In addition, large amounts of snow were deposited on the site in January. This snow effected the operation of the collectors as up to one third of the collector array was covered during the month of January. Maintenance personnel cleared the collectors in late January and the solar energy system performance was improved.

TABLE 5.1-1

WEATHER CONDITIONS

Month	Daily Incident Solar Energy Per Unit Area (50° Tilt) (Btu/ft^2-day)		Ambient Temperature (°F)		Heating Degree-Days		Cooling Degree-Days	
	Measured	Long-Term Average	Measured	Long-Term Average	Measured	Long-Term Average	Measured	Long-Term Average
Sep 78	1,416	1,448	63	60	191	166	66	15
Oct 78	1,220	1,258	48	50	557	465	0	0
Nov 78	858	852	37	35	845	891	0	0
Dec 78	767	681	21	23	1,372	1,316	0	0
Jan 79	1,090	860	10	17	1,730	1,476	0	0
Feb 79	1,392	1,133	13	20	1,458	1,253	0	0
Mar 79	1,062	1,368	31	30	1,063	1,085	0	0
Apr 79	1,178	1,440	40	44	744	623	0	3
Total	--	--	--	--	7,960	7,275	66	18
Average	1,123	1,130	33	35	995	909	8	2

5.2 System Thermal Performance

The thermal performance of a solar energy system is a function of the total solar energy collected and applied to the system load. The total system load is the sum of the energy requirements, both solar and auxiliary thermal, for each subsystem. The portion of the total load provided by solar energy is defined to be the solar fraction of the load. This solar fraction is the measure of performance for the solar energy system when compared to design or expected solar contribution.

The thermal performance of the Northview Elementary School (Howard's Grove) solar energy system is presented in Table 5.2-1 and Table 5.2-2. This performance assessment is based on the eight-month period from September 1978 through April 1979.

During the eight-month reporting period, a total of 101.03 million Btu of solar energy was collected and the total controlled system demand load was 468.84 million Btu. The measured amount of controlled solar energy delivered to the space heating load was 76.59 million Btu, which was 44 percent less than the expected value. The measured system solar fraction of 16 percent was below the expected value of 29 percent. This lower than predicted performance is due to the low performance of the collector array subsystem and to the unusual weather and solar energy system operating conditions during the reporting period. The circulating fan and losses from the rock bed also contributed 22.83 million Btu and 54.58 million Btu, respectively, to the space heating load. Thus, the net system demand load was 550.81 million Btu with solar contributing 99.44 million Btu with a resultant solar fraction of 18 percent.

The solar energy system COP (defined as the total solar energy delivered to the load divided by the total solar energy system operating energy) was 4.52 for the eight-month period. The collector array subsystem COP and the space heating subsystem solar COP for the total period were 23.37 and 6.23, respectively. These values again relate the amount of solar energy required to operate the solar portion of that subsystem. As such, the COP serves as an indicator of both how well the system was designed and how well it operated.

TABLE 5.2-1

SYSTEM THERMAL PERFORMANCE

Month	Solar Energy Collected (Million Btu)	System Load (Million Btu)	Solar Energy Used (Million Btu)		Solar Fraction (Percent)	
			Expected	Measured	Expected	Measured
Sep 78	6.16	5.29	7.3	5.13	100	97
Oct 78	13.79	19.83	19.8	3.91	100	20
Nov 78	10.68	47.45	13.1	5.46	28	12
Dec 78	10.29	88.57	8.6	9.00	10	10
Jan 79	3.82	107.22	19.3	3.61	18	3
Feb 79	19.24	90.98	27.2	18.15	30	20
Mar 79	17.28	66.88	19.2	15.40	29	23
Apr 79	19.77	42.62	21.3	15.93	50	35
Total	101.03	468.84	135.8	76.59	--	--
Average	12.63	58.61	16.98	9.37	29	16

TABLE 5.2-2

SOLAR ENERGY SYSTEM COEFFICIENTS OF PERFORMANCE

Month	Solar Energy System COP	Collector Array Subsystem COP	Space Heating Subsystem Solar COP
Sep 78	2.25	29.18	2.48
Oct 78	1.88	12.91	3.87
Nov 78	3.60	19.48	5.64
Dec 78	4.74	22.82	6.21
Jan 79	5.68	20.09	8.11
Feb 79	6.15	26.79	8.14
Mar 79	6.46	29.74	8.55
Apr 79	5.12	25.97	6.90
Total Period	4.52	23.37	6.23

At the Northview Elementary School (Howard's Grove) site, the solar energy supplied to the total load is the same as the solar energy supplied to the to the space heating load, and this is the reason that the overall system COP is less than the space heating COP. The low space heating COP suggests that the solar contribution to space heating is somewhat low.

It is interesting to note the strong influence that the local weather conditions had on the measured solar fraction. For example, the measured average outdoor ambient temperature in both January 1979 and February 1979 was seven degrees below the long-term average. In January, the measured insolation was 27 percent above the long-term average and the measured solar fraction was 3 percent. However, in February, the measured insolation was 23 percent above the long-term average and the measured solar fraction was 20 percent. In March 1979, the measured insolation was 22 percent below the long-term average, but the measured average outdoor ambient temperature of 31°F was one degree above the long-term average and the measured solar fraction was 35 percent. This is exactly what would be expected because, even though the insolation was low, the measured average outdoor ambient temperature for March was 19°F above that noted for the January-February time period. The difference in performance between January and February, even though weather conditions were similar, is attributed to the performance reduction of the collector array subsystem due to large amounts of snow. These observations serve to reinforce the statement in the Performance Assessment section concerning the impact of prevailing weather conditions on the performance of a solar energy system.

5.3 Subsystem Performance

The Northview Elementary School (Howard's Grove) solar energy installation may be divided into three subsystems:

1) Collector array
2) Storage
3) Space heating.

Each subsystem is evaluated by the techniques defined in Section 4 and is numerically analyzed each month for the monthly performance reports. This section presents the results of integrating the monthly data available on the three subsystems for the period September 1978 through April 1979.

5.3.1 Collector Array Subsystem

Collector array performance is described by comparison of the collected solar energy to the incident solar energy. The ratio of these two energies represents the collector array efficiency which may be expressed as

$$\eta_c = Q_s/Q_i \qquad (1)$$

where: η_c = Collector Array Efficiency (CAREF)

Q_s = Collected Solar Energy (SECA)

Q_i = Incident Solar Energy (SEA).

The gross collector array area is 2,685 square feet. The measured monthly values of incident solar energy, collected solar energy, and collector array efficiency are presented in Table 5.3.1-1.

Evaluation of collector efficiency using operational incident energy and compensating for the difference between gross collector array area and the gross collector area yields operational collector efficiency. Operational collector efficiency, η_{co}, is computed as follows:

$$\eta_{co} = Q_s / \left(Q_{oi} \times \frac{A_p}{A_a} \right) \qquad (2)$$

where: Q_s = Collected Solar Energy (SECA)

Q_{oi} = Operational Incident Energy (SEOP)

Q_p = Gross Collector Area (product of the number of collectors and the total envelope area of one unit) (GCA)

A_a = Gross Collector Array Area (total area perpendicular to the solar flux vector including all mounting, connecting and transport hardware (GCAA).

Note: The ratio $\frac{A_p}{A_a}$ is typically 1.0 for most collector array configurations.

TABLE 5.3.1-1

COLLECTOR ARRAY PERFORMANCE

Month	Incident Solar Energy (Million Btu)	Collected Solar Energy (Million Btu)	Collector Array Efficiency	Operational Incident Energy (Million Btu)	Operational Collector Efficiency
Sep 78	114.07	6.16	0.05	21.61	0.29
Oct 78	101.57	13.79	0.14	90.00	0.15
Nov 78	69.17	10.68	0.15	53.52	0.20
Dec 78	63.89	10.29	0.16	41.49	0.25
Jan 79	90.79	3.82	0.04	19.30	0.20
Feb 79	104.70	19.24	0.18	77.73	0.25
Mar 79	88.46	17.28	0.20	58.52	0.30
Apr 79	94.93	19.77	0.21	66.73	0.30
Total	663.69	101.03	--	428.90	--
Average	82.96	12.63	0.15	53.61	0.24

This latter efficiency term is not the same as collector efficiency as represented by the ASHRAE Standard 93-77 [5]. Both operational collector efficiency and the ASHRAE collector efficiency are defined as the ratio of actual useful energy collected to solar energy incident upon the collector and both use the same definition of collector area. However, the ASHRAE efficiency is determined from instantaneous evaluation under tightly controlled, steady-state test conditions, while the operational collector efficiency is determined from the actual conditions of daily solar energy system operation. Measured monthly values of operational incident energy and computed values of operational collector efficiency are also presented in Table 5.3.1-1.

Collector array efficiency may be viewed from two perspectives. The first assumes that the efficiency be based upon all available solar energy; however, that point of view makes the operation of the control system a part of array efficiency. For example, energy may be available at the collector, but the collector fluid temperature is below the control minimum, thus the energy is not collected. The monthly efficiency computed by this method is listed in the column entitled "Collector Array Efficiency" in Table 5.3.1-1.

The second viewpoint assumes the efficiency be based upon only the incident energy during periods of collection. The monthly efficiency computed by this method is listed in the column entitled "Operational Collector Array Efficiency." Efficiency computed by this method is used in the following discussion.

The Northview Elementary School (Howard's Grove) collector array consists of 138 Sun Stone flat-plate air collectors arranged in six parallel rows. Within each row there are 23 parallel collector panels. This arrangement is shown schematically in Figure 5.3.1-1. Table 5.3.1-2 presents a comparison of the actual performance of the collector array for the month of February (February was chosen as the example month because the measured insolation was 23 percent above the long-term average and the collector array was operational on 24 of 28 days during the month) against four predictions of performance which are based on instantaneous efficiency curves.

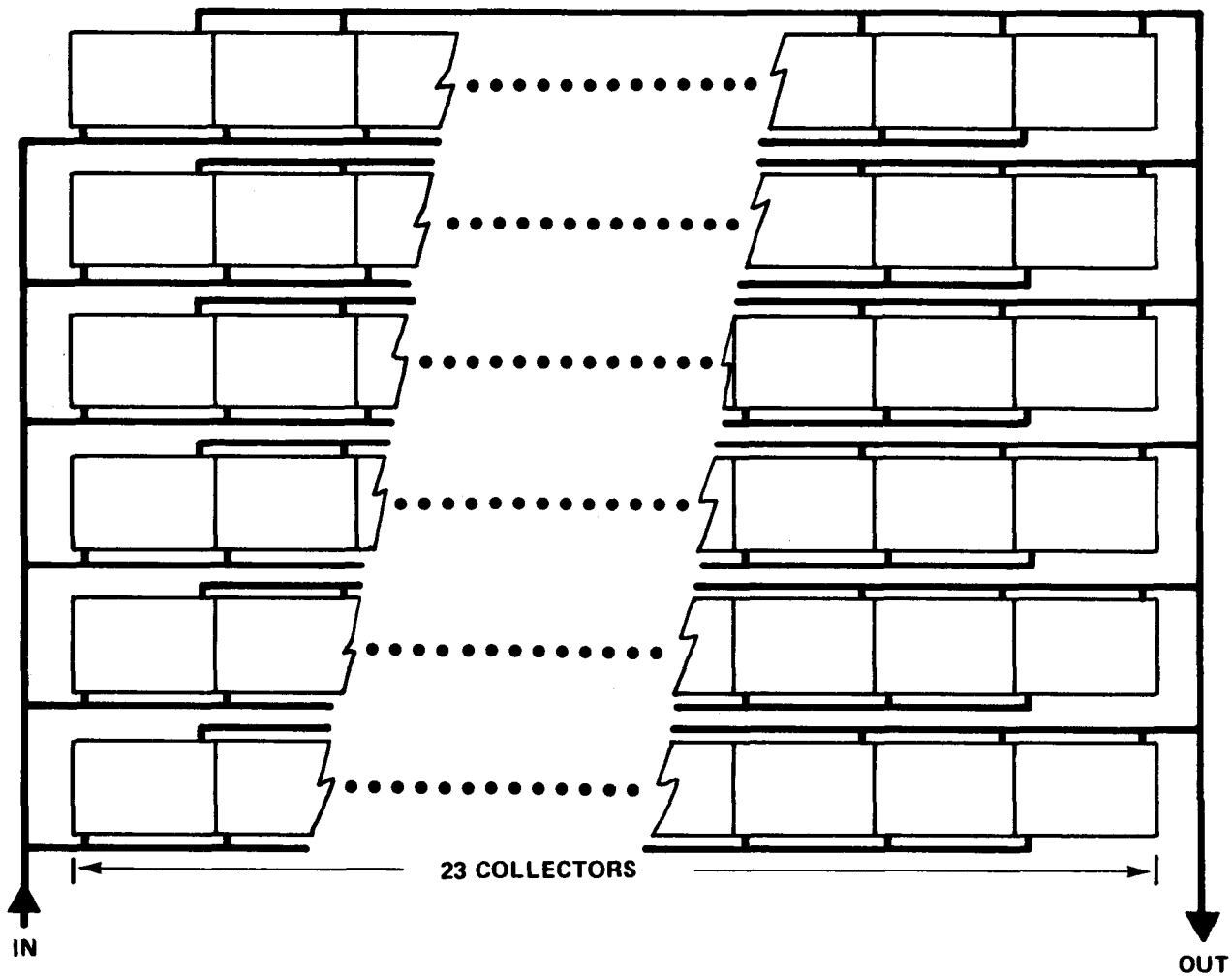

FIGURE 5.3.1-1 COLLECTOR ARRAY ARRANGEMENT

TABLE 5.3.1-2

ENERGY GAIN COMPARISON
FEBRUARY

SITE: EDWARDS GROVE SCHOOL EDWARDS GROVE, WIS

DAY	ACTUAL	ERROR			
		FIELD DERIVED			LAB
		MONTH	LONG TERM	2ND ORDER	PANEL
1	1.367E+06	-0.130	-0.120	-0.124	-0.070
2	5.438E+05	0.064	0.078	0.045	0.228
3	6.626E+05	0.016	0.030	0.000	0.230
4	8.538E+05	-0.317	-0.309	-0.312	-0.238
5	2.139E+05	-0.226	-0.215	-0.245	-0.022
6	0.000E+00	0.000	0.000	0.000	0.000
7	6.073E+05	-0.293	-0.285	-0.289	-0.214
8	1.256E+06	-0.173	-0.163	-0.172	-0.070
9	1.130E+06	-0.183	-0.173	-0.177	-0.104
10	1.026E+06	-0.023	-0.010	-0.061	0.165
11	0.000E+00	0.000	0.000	0.000	0.000
12	2.314E+05	-0.247	-0.237	-0.250	-0.107
13	3.721E+05	-0.010	0.006	-0.053	0.382
14	0.000E+00	0.000	0.000	0.000	0.000
15	0.000E+00	0.000	0.000	0.000	0.000
16	1.088E+06	-0.210	-0.201	-0.208	-0.118
17	5.164E+05	-0.203	-0.193	-0.211	-0.075
18	4.454E+05	-0.303	-0.292	-0.324	-0.074
19	1.263E+06	-0.133	-0.123	-0.123	-0.095
20	1.236E+06	-0.096	-0.090	-0.094	-0.102
21	2.019E+05	-0.420	-0.413	-0.421	-0.341
22	3.648E+05	-0.048	-0.038	-0.044	-0.004
23	7.103E+05	-0.183	-0.175	-0.182	-0.183
24	7.400E+05	-0.213	-0.202	-0.225	-0.038
25	1.121E+06	-0.095	-0.086	-0.089	-0.046
26	1.349E+06	0.139	0.149	0.125	0.269
27	1.580E+06	0.113	0.123	0.119	0.138
28	3.605E+05	0.147	0.165	0.078	0.579
	1.925E+07	-0.123	-0.113	-0.127	-0.028

CURVE	COEFFICIENTS			
	AO (FRIA)	A1 (FRUL)	A2 (*)	R**2
PANEL	0.500	-0.990	N.A.	N.A.
MONTH	0.422	-0.429	N.A.	0.048
LTIST	0.419	-0.437	N.A.	0.085
LT2ND	0.482	-0.839	1.168	N.A.

Instantaneous efficiency curves are derived from laboratory test data supplied by the collector manufacturer and from three empirical sources: a linear regression line fit through field data obtained in February; a linear regression line fit through all field data in the base; and a curvilinear (second order) regression line fit through all field data in the base (the base data consists of all measurements relating to collector array performance made from December 1978 through April 1979). The collector array performance for September through November was degraded due to a half-closed fire damper door.

Each error value presented in the error field of Table 5.3.1-2 is computed by the equation

$$\text{error} = (A - P)/P \qquad (3)$$

where:

A is the actual energy gain of the collector array shown in column one (million Btu/day)

P is the predicted energy gain of the collector array based on projecting the measured operating point to the applicable instantaneous efficiency curve and multiplying by the measured insolation level and collector array area and then summing over all the measured operating points (million Btu/day).

The computed error is then a measure of how well the particular prediction curve fits the reality of dynamic operating conditions in the field.

The results in Table 5.3.1-2 indicate that the actual collector energy gain performance was 12 percent below that which would have been expected from projecting the measured operating point on the instantaneous efficiency curve derived from field data for the month of February. The actual

collector energy gain performance was 10 percent below that expected from using the long-term instantaneous efficiency curve derived from the data base December 1978 through April 1979. However, the energy gain comparison between laboratory test data and the actual collector array shows relatively good agreement (within three percent). These results suggest that February collector performance exhibits a lot of scatter which is substantiated by the low coefficient of determination (R^{**2}) of 0.086. Also, other factors must be affecting monthly collector array performance other than the collector array itself. It should also be noted that the manufacturer's single-panel curve provides a prediction accuracy of 2.8 percent, which is exceptionally close to the actual energy gain.

Figure 5.3.1-2 presents a histogram of the collector array operating points for February. Also presented in Figure 5.3.1-2 are linear instantaneous efficiency curves based on controlled laboratory test data supplied by the collector manufacturer, field data for the month of February and long-term field data for the base period. In addition the collector efficiency at the dominant operating point and the actual monthly collector array performance are indicated on the figure. The ordinate of the graph shown in Figure 5.3.1-2 has a printed range of 0 to 10 percent to display the distribution of collector array operating points. However, the value printed on the ordinate should be multiplied by 10 when the intercepts of the linear instantaneous efficiency curves are being evaluated (these values range from 0 to 100 percent).

The collector array operating points, X, are calculated each scan by the equation

$$X = (T_{f,i} - T_a)/I \qquad (4)$$

where:

$T_{f,i}$ is the inlet temperature of the collector array transport fluid (°F)

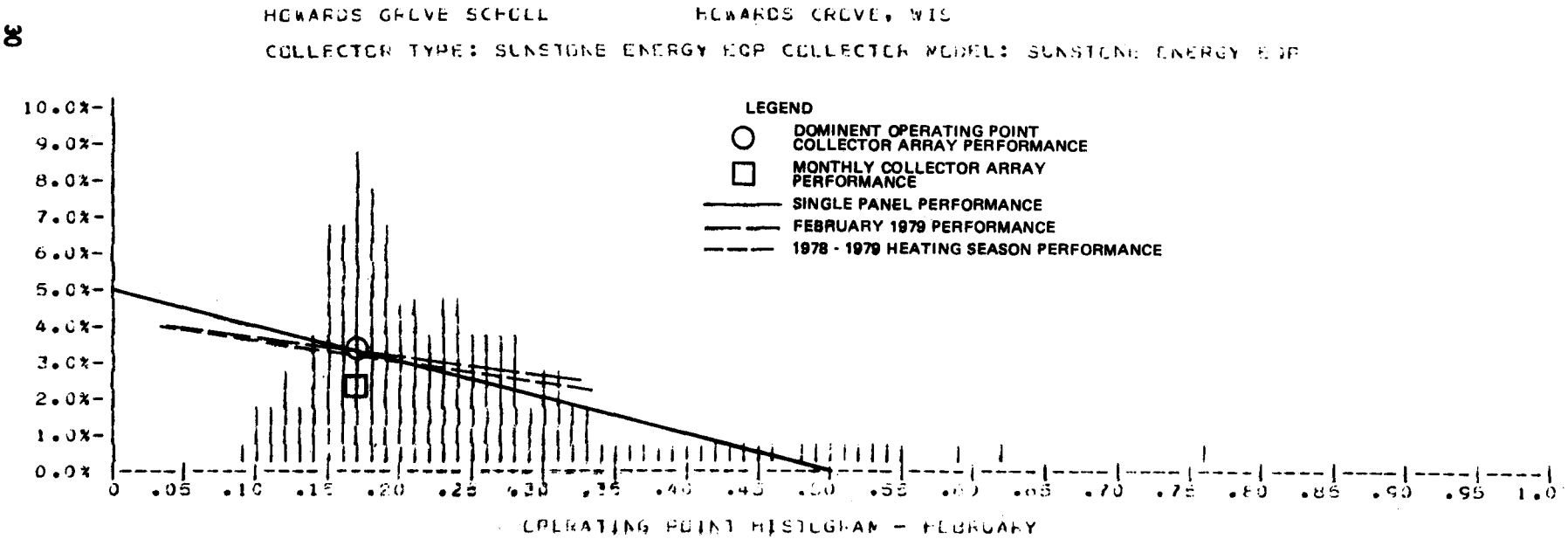

AIR PROPERTIES

AVERAGE LOCAL BAROMETRIC PRESSURE 14.40 PSI

AVERAGE LOCAL RELATIVE HUMIDITY 72.00

AVERAGE TEMPERATURE 32.00 DEGR FAHRENHEIT

ARRAY FLOW RATE 265.00 CUBIC FEET/MIN

PANEL FLOW RATE 155.33 CUBIC FEET/MIN

AVERAGE TEMPERATURE GAIN 41.65 DEGR FAHRENHEIT

LONG TERM CURVE FIT VALID FROM 0.080 TO 0.256

FIGURE 5.3.1-2 COLLECTOR ARRAY OPERATING POINT HISTOGRAM AND INSTANTANEOUS EFFICIENCY CURVES

T_a is the temperature of the ambient air (°F)

I is the insolation rate (Btu/ft^2-hr).

Examination of the operating point histogram indicates that the predominant region of collector array operation occurred for operating points between 0.15 to 0.24 (62 percent of the time). This leads to the expectation that the operational collector array efficiency would typically be on the order of 0.36, which is somewhat higher than the monthly collector array performance indicated in Figure 5.3.1-2 and presented in Table 5.3.1-1. The cause of the lower monthly collector array efficiency indicated for February is not readily apparent from these results.

Table 5.3.1-3 contains the annual energy gain comparison for all the data in the data base period December 1978 through April 1979. The long-term results are in close agreement with the results obtained in February 1979.

Analysis of the collector array performance for the spring months revealed that collector leakage exists. The inlet and outlet collector air flow sensors indicate that the leakage air flow is into the collector array. Air leaks into the outlet ducting of the collector array tend to reduce collector efficiency. Air leaks at the inlet or along the collector array tend to increase collector efficiency [7].

When air leaks or infiltrates into collectors, the energy required to heat this air may generally be regarded as a loss. This results from the law of conservation of mass which requires that somewhere in the air circuit the leakage flow into the collector must be balanced by an outflow at temperatures greater than the inlet flow. However, in many cases, ambient air must be introduced to satisfy fresh air requirements. This is the case at the Northview Elementary School (Howard's Grove). Here, the leakage does not represent a loss. The collector, acting partly as a fresh air preheater, actually supplies fresh air to the load.

TABLE 5.3.1-3

ENERGY GAIN COMPARISON
(ANNUAL)

SITE: HOWARDS GROVE SCHELL HOWARDS GROVE, WIS

			ERROR			
			FIELD DERIVED			LAE
MONTH	YEAR	ACTUAL	MONTH	LONG TERM	2ND ORDER	PANEL
JANUARY	79	3.738E+06	-0.164	-0.253	-0.284	-0.155
FEBRUARY	79	1.925E+07	-0.123	-0.104	-0.125	-0.029
MARCH	79	1.695E+07	-0.186	-0.071	-0.034	0.029
APRIL	79	1.957E+07	-0.091	-0.109	-0.074	-0.060
MAY		0.000E+00	0.000	0.000	0.000	0.000
JUNE		0.000E+00	0.000	0.000	0.000	0.000
JULY		0.000E+00	0.000	0.000	0.000	0.000
AUGUST		0.000E+00	0.000	0.000	0.000	0.000
SEPTEMBER		0.000E+00	0.000	0.000	0.000	0.000
OCTOBER		0.000E+00	0.000	0.000	0.000	0.000
NOVEMBER		0.000E+00	0.000	0.000	0.000	0.000
DECEMBER	78	9.311E+06	-0.053	-0.053	0.007	0.043
AVERAGE		1.360E+07	-0.122	-0.104	-0.074	-0.020

CURVE	COEFFICIENTS			
	A0 (BETA)	A1 (PROD)	A2 (*)	R**2
PANEL	0.800	-0.990	N.A.	N.A.
MONTH	0.431	-0.349	N.A.	0.011
LT1ST	0.467	-0.573	N.A.	0.113
LT2ND	0.354	1.116	-0.719	N.A.

The collector leakage effects on collector efficiency with air leaking in are expressed by the following equations [7]:

$$\eta_L^+ = F_{RL}^+ \left[(\alpha\tau)_e - U_L \left\{ 1 + \frac{G_L}{G_i} \times G_i C_p / U_L \times (1/F' - 1/F_{RL}^+) \right\} (T_{f,i} - T_a) / I \right] \quad (5)$$

$$F_{RL}^+ = \frac{\left[1 - \exp \left\{ (1 + \frac{G_i}{G_L} \cdot F' U_L / G_i C_p) \ln \left(\frac{1}{1 + G_L/G_i} \right) \right\} \right]}{\left[\frac{U_L}{G_i C_p (1 + G_L/G_i)} \cdot \left\{ 1 + G_L/G_i \cdot G_i C_p F'/U_L \right\} \right]} \quad (6)$$

where

η_L^+ is the collection efficiency of collector with air leaking in

η is the collection efficiency without taking air leaks into account

C_p is the specific heat of air

F_{RL}^+ is the collector heat removal factor when air leaks in

F' is the collector efficiency factor

G_i is the collector inlet air mass flow per unit collector area

G_L is the collector leakage air mass flow per unit collector area

U_L is the overall collector heat loss coefficient.

Using the predicted collector array performance parameters obtained from laboratory test data and actual measured collector leakage, as indicated by the difference between the air flow at the inlet to the collector array and the air flow at the inlet to rock storage, two collector leakage instantaneous performance curves can be generated.

Collector leakage during the winter months is approximately 8.8 percent which results in an efficiency curve equation of

$$\eta_L^+ \ (8.8\%) = 0.592 \ [0.9 - 1.711 \ (T_{f,i} - T_a)/I]. \quad (7)$$

This curve is shown on Figure 5.3.1-3.

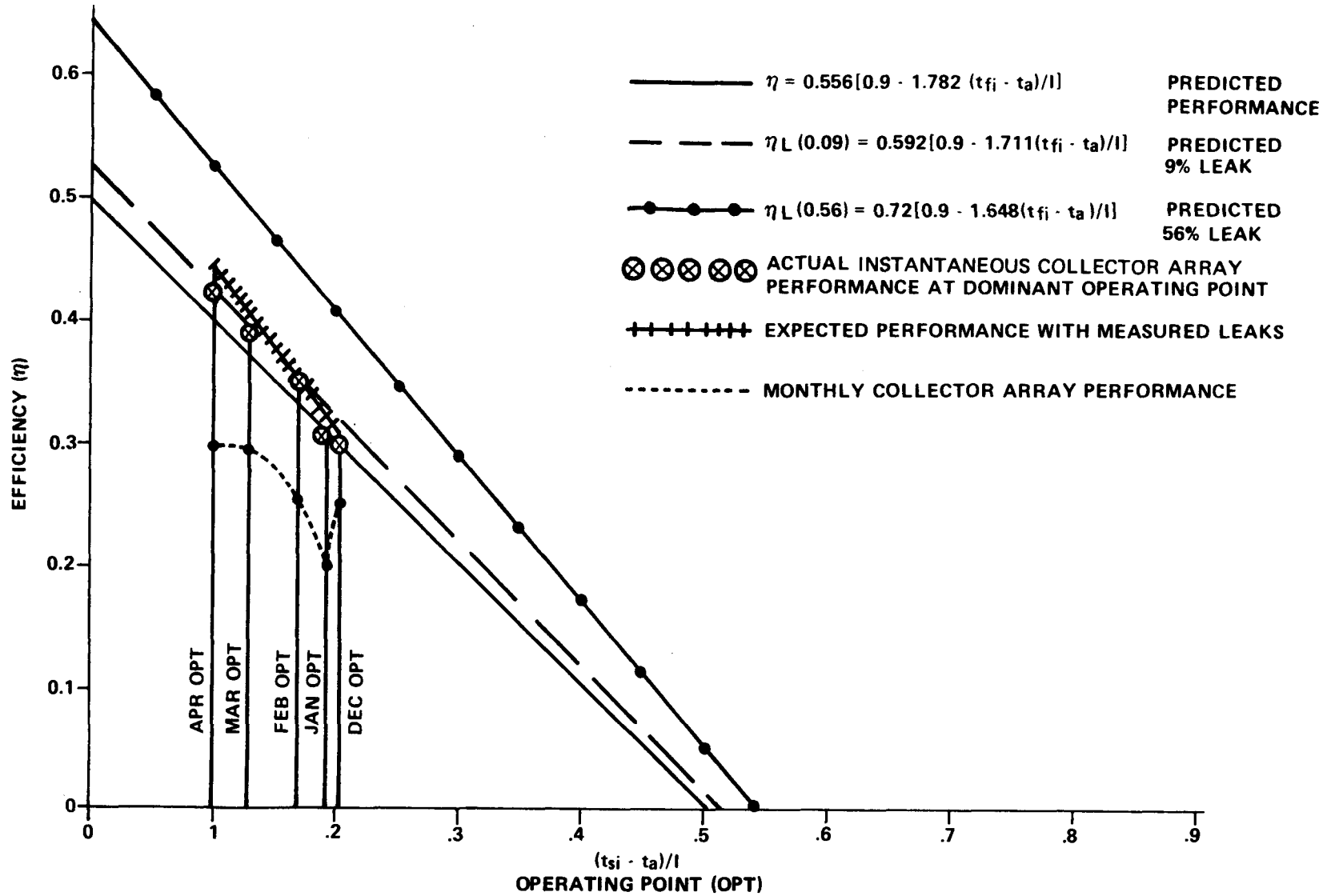

FIGURE 5.3.1-3 COMPARISON OF COLLECTOR ARRAY PERFORMANCE PREDICTIONS AND ACTUAL COLLECTOR ARRAY PERFORMANCE

Collector leakage during spring months is similar to that in winter when the site is occupied but increases when the solar control system shifts to the unoccupied mode and solar energy collection is still in progress. The leakage indication in the unoccupied mode is approximately 56 percent. The efficiency curve equation becomes

$$\eta_L^+ (56\%) = 0.72\ [0.9 - 1.648\ (T_{f,i} - T_a)/I] \qquad (8)$$

which is also shown in Figure 5.3.1-3.

Figure 5.3.1-3 illustrates the comparison of collector array instantaneous efficiency performance predictions from laboratory test data, for the 8.8 percent leakage case, for the 56 percent leakage case, and the expected collector array performance taking into account actual measured leakage and predicted laboratory performance. Also included in Figure 5.3.1-3 are the actual instantaneous collector array performance indicated at the dominant operating point for each month and the monthly collector array performance from Table 5.3.1-1.

The actual collector performance at the dominant operating point each month agrees very well with the expected performance of the collector array in the presence of air leakage into the collector array. This result tends to substantiate that collector air leakage exists.

The collector air leakage is actually beneficial to collector array performance. In addition, the collector array efficiency increases as the operating point moves from winter to spring (see Figure 5.3.1-3). This is consistent with an air system in which the collector return air temperature is nearly constant, which is the case for the Northview Elementary School (Howard's Grove) solar energy system. As the ambient outside temperature rises, the operating point shifts towards lower values and the collector efficiency increases. The effect is clearly illustrated in the monthly collector efficiencies of Table 5.3.1-1.

Further analysis has revealed that the cause of the low monthly operational collector efficiency is due to the operating characteristics of the collector array. Table 5.3.1-4 lists typical operating characteristics of the collector array during the reporting period, along with the number of days collection actually existed during the month.

The data in Table 5.3.1-4 indicate that collector turn-on is occurring late in the morning during winter months. Also, the collector differential temperature at turn on is on the order of 26°F, as opposed to the design value of 17°F. This effect is also substantiated by the low amount of insolation measured when the collector array was operational, as compared to the total amount of insolation available. The ratio of these quantities for the reporting period was 0.65. This is considerably lower than desired.

It appears that a significant collector thermal lag exists during collector turn on. Because of low temperatures in this area and relatively high collector losses, a considerable amount of time is required to heat the collector thermal mass in order to initiate collector turn on. This effect reduces the number of days the collectors can function in the winter months as indicated by the reduced days of operation in December 1978 and January 1979.

The alleviation of the collector operating problem would require that the U_L of the collectors be reduced and/or the collector turn-on temperature differential be reduced to allow more collection time. The reduction of the collector U_L would require the addition of another glazing or more insulation in the collector backing. Since this is an expensive proposition, another alternative should be taken. The reduction of the collector turn-on differential temperature during winter months should be considered. The low grade energy derived would be useful to the system as the building is operated at low temperatures (less than 65°F). The solar system performance could be improved by this control modification.

Additional information concerning collector array analysis in general may be found in a forthcoming paper [16] that describes collector array analysis procedures in detail and presents the results of analysis performed on numerous collector array installations across the United States.

TABLE 5.3.1-4

COLLECTOR ARRAY OPERATING CONDITIONS

Month	Time (A.M.)	Collector Array Initiation Parameters on a Typical Day During the Month			Collector Operational Days During The Month
		Differential Temperature (°F)	Insolation (Btu/Ft^2-Hr	Absorber Temperature (°F)	
Dec 78	9:34	26.6	256	143	15
Jan 79	9:33	26.6	227	140	9
Feb 79	9:28	11.0	204	138	24
Mar 79	8:30	13.0	201	130	17
Apr 79	8:15	26.0	180	127	21

5.3.2 Storage Subsystem

Storage subsystem performance is described by comparison of energy to storage, energy from storage and change in stored energy. The ratio of the sum of energy from storage and change in stored energy to energy to storage is defined as storage efficiency, η_s. This relationship is expressed in the equation

$$\eta_s = (\Delta Q + Q_{so})/Q_{si} \qquad (9)$$

where:

ΔQ = change in stored energy. This is the difference in the estimated stored energy during the specified reporting period, as indicated by the relative temperature of the storage medium (either positive or negative value) (STECH).

Q_{so} = energy from storage. This is the amount of energy extracted by the load subsystem from the primary storage medium (STEO).

Q_{si} = energy to storage. This is the amount of energy (both solar and auxiliary) delivered to the primary storage medium (STEI).

Evaluation of the system storage performance under actual transient system operation and weather conditions can be performed using the parameters listed above. The utility of these measured data in evaluation of the overall storage design can be illustrated in the derivation presented below.

The overall thermal properties of the storage subsystem design can be derived empirically as a function of storage average temperature (average storage temperature for the reporting period) and the ambient temperature in the vicinity of the storage tank.

An effective storage heat transfer coefficient (C) for the storage subsystem can be defined as follows:

$$C = (Q_{si} - Q_{so} - \Delta Q_s)/[(\bar{T}_s - \bar{T}_a) \times t] \frac{Btu}{Hr\text{-}°F} \qquad (10)$$

where

C = effective storage heat transfer coefficient

Q_{si} = energy to storage (STEI)

Q_{so} = energy from storage (STEO)

ΔQ_s = change in stored energy (STECH)

$\bar{T}_s$ = storage average temperature (TS)

$\bar{T}_a$ = average ambient temperature in the vicinity of storage (TE)

t = number of hours in the month (HM).

The effective storage heat transfer coefficient is comparable to the heat loss rate defined in ASHRAE Standard 94-77 [6]. It has been calculated for each month in this report period and included, along with Storage Average Temperature, in Table 5.3.2-1.

Examination of the values for the effective storage heat transfer coefficient shows a significant amount of scatter for the eight-month period from September 1978 through April 1979. The mean for these months was 69 Btu/hr°F, but the standard deviation (obtained using N-1 weighting) was 299 Btu/hr°F. The exact reason for this scatter is not known, but there are several factors that must be considered. First, it can be seen that the storage subsystem

TABLE 5.3.2-1

STORAGE SUBSYSTEM PERFORMANCE

Month	Energy To Storage (Million Btu)	Energy From Storage (Million Btu)	Change In Stored Energy (Million Btu)	Storage Efficiency	Storage Average Temperature (°F)	Effective Storage Heat Loss Coefficient (Btu/Hr°F)
Sep 78	6.16	5.13	-0.04	0.83	74	37
Oct 78	13.79	3.91	0.16	0.30	68	435
Nov 78	11.14	5.46	0.13	0.50	72	128
Dec 78	9.00	9.00	-0.05	0.49	68	23
Jan 79	3.51	3.61	0.68	1.05	64	-524
Feb 79	17.86	18.15	0.29	1.03	70	-122
Mar 79	16.96	15.40	-0.15	0.90	75	255
Apr 79	19.74	15.93	-0.13	0.76	82	322
Total	98.16	76.59	1.30	--	--	--
Average	12.27	9.57	0.16	0.79	72	69

operates at a fairly low temperature (72°F) as compared to a residential application. Since the desired building temperature is 67°F there exists the possibility of interactions between the building and the rock bed, with energy flow in and out depending on the solar energy available and the time of day. The rock bed-building interaction could account for the indicated variation in the effective heat transfer coefficient. The negative heat transfer coefficient may be due in part to the energy imbalance that exists. The high space heating system air flow (approximately 11,000 cfm), combined with the temperature uncertainty of 0.25°F, can contribute to the situation.

The eight-month average storage efficiency was 0.79. This indicates that the storage subsystem performed well, especially when the perturbations discussed in the preceding paragraph are considered.

Analysis of the storage subsystem revealed that its performance may be degraded because of a steel plenum barrier that was installed in the rock storage at the time of construction. Energy collected is placed in the top of rock storage between the collector inlet and the building-return vertical inlet air shaft (see "Hot Rocks" of Figure 5.3.2-1). However, when energy is removed from rock storage, the air flow path is from the bottom of rock storage, then to the outlet leading to the supply duct. This path does not pass through the portion of the rock that was heated by the collectors (see "Cool Rock" of Figure 5.3.2-1). The temperature profile of the interior storage sensors verifies that this condition exists. Only temperatures T200, T201, and T202 (top storage temperatures) show any significant temperature rise when solar energy is being collected. The remaining temperatures are stable in the region of 66°F to 72°F. Some of the energy in the hot region is believed to migrate to the cooler rocks. However, a considerable amount of time is required for migration of the energy in the hot region to the rock bed outlet. In spring, the rock bed temperatures in the hot region are greater than 100°F but temperatures in the cool region are less than 85°F. This condition results in auxiliary consumption during morning hours in spring because of the requirement for a supply temperature of 95°F. A better situation may have been obtained if the storage plenum barrier did not exist.

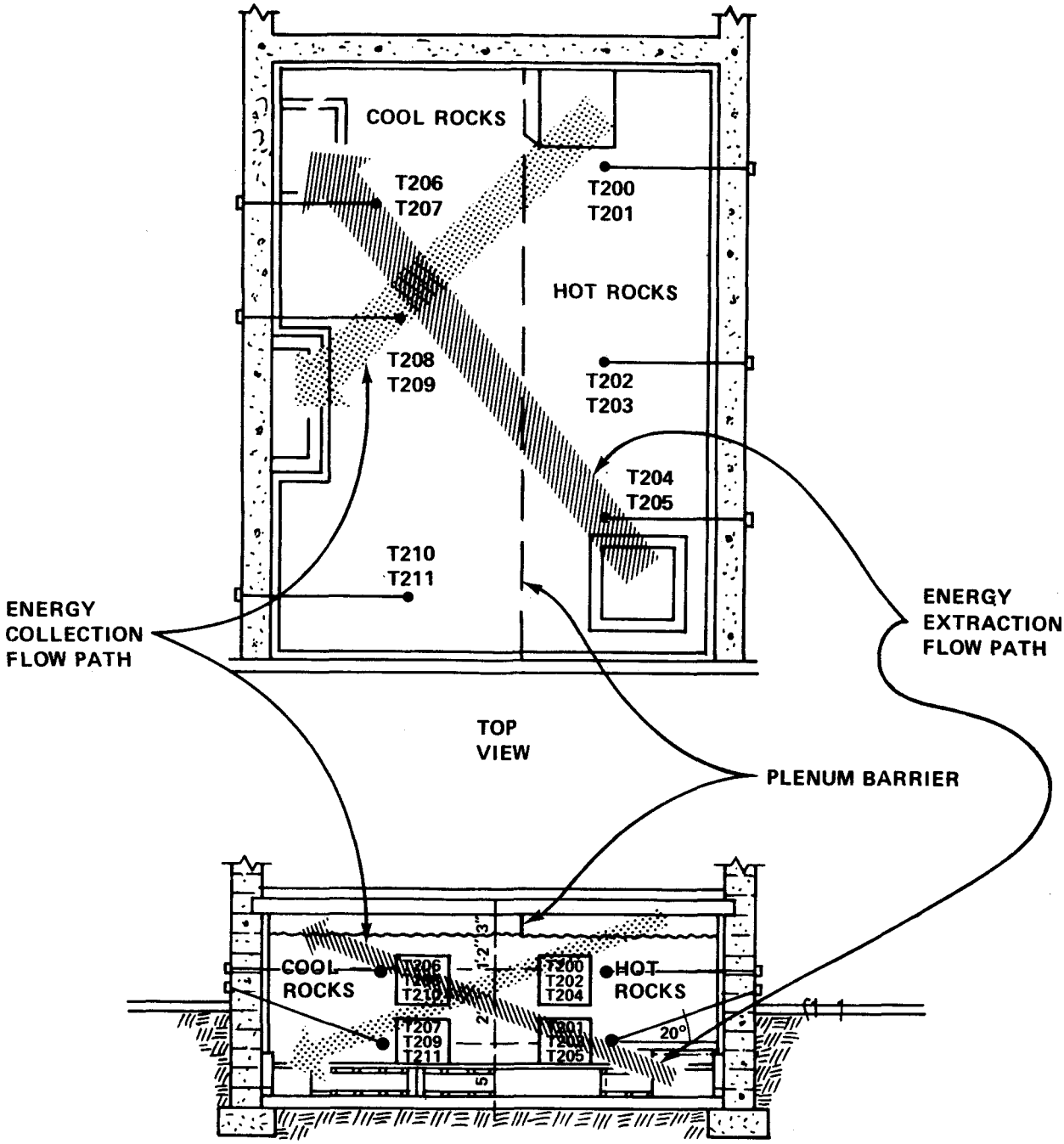

FIGURE 5.3.2-1 ROCK STORAGE BED ENERGY FLOW PATHS

5.3.3 Space Heating Subsystem

The performance of the space heating subsystem is described by comparing the amount of solar energy supplied to the subsystem with the energy required to satisfy the total space heating load. The energy required to satisfy the total load consists of both solar energy and auxiliary thermal energy. The ratio of solar energy supplied to the load to the total load is defined as the heating solar fraction. The calculated heating solar fraction is the indicator of performance for the subsystem because it defines the percentage of the total space heating load supported by solar energy.

The performance of the Northview Elementary School (Howard's Grove) space heating subsystem is presented in Table 5.3.3-1. For the eight-month period from September 1978 through April 1979, controlled solar energy supplied a total of 76.49 million Btu to the space heating load. The total controlled heating load for this period was 468.84 million BTU, and the average monthly controlled solar fraction was 16 percent. The remainder of the space heating load was supplied by 393.06 million Btu of auxiliary fossil fuel (2,722 gallons of fuel oil). The system performance was somewhat low in January 1979, but this is a direct result of significant deviations of weather conditions from the climatic norm. During this month the average outdoor ambient temperature was seven degrees below normal and the measured insolation in the plane of the collector array was 29 percent above the long-term average. As noted in the Summary and Conclusions seciton of this report, snowfall (and hence cloudy weather) was much higher than normal during January. Snow covered anywhere from 30 percent to 100 percent of the collector array during January and this, combined with a collector array control set point problem, prevented the collector array from functioning properly in January. The collector array only operated on 9 of 31 days during the month of January.

Analysis of the performance of the rock bed revealed that the large 7.5 HP circulating fan added energy to the building circulation air flow. This energy produced a 1.5°F temperature rise across the circulation fan,

TABLE 5.3.3-1

HEATING SUBSYSTEM PERFORMANCE

Month	Space Heating Load (Million Btu)		Energy Consumed (Million Btu)				Measured Solar Fraction (Percent)	
			Solar					
	Controlled	Uncontrolled*	Controlled	Uncontrolled*	Auxiliary Thermal	Auxiliary	Controlled	Uncontrolled* + Controlled
Sep 78	5.29	1.94	5.13	1.03	0.16	0.21	97	85
Oct 78	19.83	13.92	3.71	9.72	15.92	20.95	20	40
Nov 78	47.45	11.86	5.46	5.55	41.99	55.25	12	19
Dec 78	88.57	11.44	9.00	0.05	79.56	108.68	10	9
Jan 79	107.22	12.71	3.61	0	103.61	136.61	3	3
Feb 79	90.98	7.57	18.18	0	72.84	95.84	20	18
Mar 79	66.98	7.48	15.40	1.71	51.48	67.74	23	23
Apr 79	42.62	10.49	15.93	4.77	27.50	36.18	35	39
Total	468.84	77.41	76.59	22.83	393.06	517.18	--	--
Average	58.61	9.68	9.57	2.85	49.13	64.65	16	18

* Uncontrolled energy gains are derived from two sources:
(1) circulating fan air disturbances that raised the temperature of the circulating air and contributed to rock bed temperature stabilization;
(2) rock bed losses to the mechanical room and building.

and thus contributed to satisfying the space heaitng demand. The magnitude of the induced energy amounted to 48.86 million Btu during the reporting period.

The solar energy system rock thermal storage bed is located under the mechanical room inside the school. Energy leaking from the rock bed has been noted in the mechanical room. This energy is assume to have also contributed to the space heating demand. The magnitude of the rock bed losses were 22.83 million Btu for the reporting period.

The total space heating demand rises to 556.25 million Btu when the rock bed losses and fan induced energy are added to the controlled space heating demand. The solar energy contribution is then 99.42 million Btu, which results in a overall solar fraction of 18 percent.

The instrumentation at Northview School (Howard's Grove) allows the determination of the space heating demand from three different sets of sensors. One sensor set uses absolute temperatures and circulation air flow measurements (Figure 3-1, W400, W403, W402, T600 and T650). Another set of sensors utilizes absolute temperatures and liquid flow measurements (Figure 3-1, W401, T401 and T451) associated with the liquid-to-air heat exchanger used to transfer furnace energy to the building. The last set of sensors use a burner on/off measurement (Figure 3-1, EP406) and measured furnace efficiencies.

A comparison of the space heating demand computed from each sensor set is shown in Figure 5.3.3-1. Also included in the figure is the Department of Energy supplied estimate of the space heating demand. The design heating load was calculated by assuming that a large controlled infiltration of outside air exists during normal operation of the site. The actual infiltration apparently was lower than expected. Therefore, a better method of determining the predicted space heating load had to be devised. The method chosen was to use the building heat loss coefficient (UA)

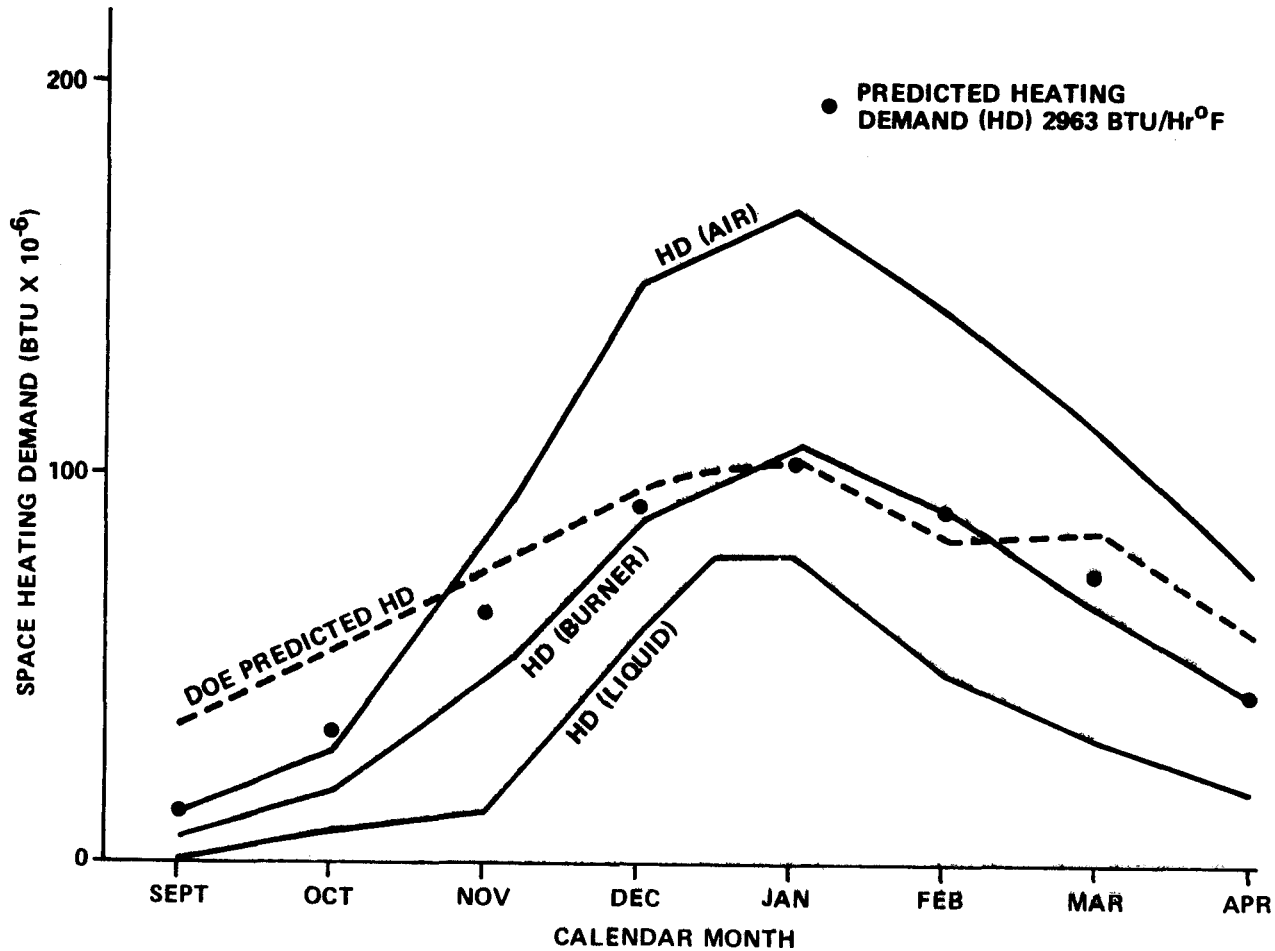

FIGURE 5.3.3-1 COMPARISON OF MEASURED VERSUS PREDICTED HEATING DEMAND

computed using the predicted design loads for December 1978, January 1979 and February 1979 when little outside air infiltration exists. The computed UA for the period was 2,963 Btu/day-°F. The space heating demand estimated using this building heat transfer coefficient is also shown in Figure 5.3.3-1.

The data shown in Figure 5.3.3-1 indicate a large discrepancy between the space heating demand as computed by the three methods. Detailed discussions with design personnel at the site and actual fuel oil consumption data supplied by the school reveal that computations using the burner instrumentation set most closely approximate the actual space heating demand at the site. Therefore, all the results presented in the monthly reports written for this site and the results presented in this System Performance Evaluation Report utilize the burner data as the "true" indication of the space heating demand.

5.4 Operating Energy

Operating energy for the Northview Elementary School (Howard's Grove) solar energy system is defined as the energy required to transport solar energy to the point of use. Total operating energy for this system consists of energy collection and storage subsystem operating energy and space heating subsystem operating energy. Operating energy is electrical energy that is used to support the subsystems without affecting their thermal state. Measured monthly values for subsystem operating energy are presented in Table 5.4-1.

Total system operating energy for the Northview Elementary School (Howard's Grove) is the electrical energy required to operate the building circulation fan, the collector array circulation fan, the auxiliary heat transfer pump and the burner power indication. These are shown in Figure 3-1 as EP402, EP403, and EP406, respectively. Although additional electrical energy is required to operate the motor driven dampers shown in Figure 3-1 and the control system for the installation, it is not included in this report. These devices are not monitored for power consumption and the power they consume is inconsequential when compared to the fan motor.

The large operating energy indicated is due principally to the 7.5 HP circulation fan. The circulation fan distributes both solar and auxiliary energy to the space heating load. Therefore, the solar electrical operating energy is computed by multiplying the solar fraction times the fan energy, and this amounted to 13.49 million Btu. Thus, for every one million Btu of solar energy delivered to the load, 0.14 million Btu (or 40 kwh) of electrical operating energy was expended to operate the solar system.

TABLE 5.4-1

OPERATING ENERGY

Month	ECSS Operating Energy (Million Btu)	Space Heating Operating Energy (Million Btu)	Total System Operating Energy (Million Btu)
Sep 78	0.21	2.13	2.33
Oct 78	1.07	5.06	6.13
Nov 78	0.55	8.07	8.62
Dec 78	0.45	14.49	14.94
Jan 79	0.19	14.84	15.03
Feb 79	0.72	11.15	11.87
Mar 79	0.58	7.83	8.41
Apr 79	0.76	6.25	7.61
Total	4.53	69.82	79.94
Average	0.57	8.73	9.37

5.5 Energy Savings

Solar energy system savings are realized whenever energy provided by the solar energy system is used to meet system demands which would otherwise be met by auxiliary energy sources. The operating energy required to provide solar energy to the load subsystem is subtracted from the solar energy contribution, and the resulting energy savings are adjusted to reflect the coefficient of performance (COP) of the auxiliary source being supplanted by solar energy.

The auxiliary energy source is a fuel oil furnace located in the mechanical room. Energy from the furnace is delivered to a liquid-to-air heat exchanger located in the building supply duct downstream of the thermal rock storage bed. The circulation fan delivers the energy from both the auxiliary furnace and the rock storage bin to the building.

Electrical energy savings for September 1978 through April 1979 are presented in Table 5.5-1. For this time period, the sum of the average gross controlled and uncontrolled monthly savings was 16.21 million Btu. After the total system operating energy was deducted the average net monthly savings were 12.45 million Btu, or 86 gallons of fuel oil. For the overall time period covered by this report the total net savings were 99.69 million Btu, or 691 gallons of fuel oil ($324.77 at 47 cents per gallon).

TABLE 5.5-1

ENERGY SAVINGS

Month	Fossil Energy Savings Space Heating (Million Btu)		Fuel Oil Savings (Gallons)	Solar Operating Energy (Million Btu)	Electrical Savings		Fossil Equivalent At Source (Million Btu)
	Controlled	Uncontrolled			Million Btu	kwh	
Sep 78	6.75	1.35	46.7	2.33	-2.33	-683	-7.76
Oct 78	5.15	12.78	36.7	3.52	-3.52	-1,031	-11.72
Nov 78	7.18	7.30	49.7	4.08	-4.08	-1,195	-13.59
Dec 78	11.85	0.06	82.1	5.50	-5.50	-1,611	-18.32
Jan 79	4.75	0.0	32.9	6.47	-6.47	-1,896	-21.55
Feb 79	23.88	0.0	165.4	3.41	-3.41	-999	-11.36
Mar 79	20.26	2.25	140.3	2.30	-2.30	-674	-7.66
Apr 79	19.87	6.28	137.6	2.44	-2.44	-715	-8.13
Total	99.69	30.02	691.4	30.05	-30.05	-8,804	-100.09
Average	12.46	3.75	86.4	3.76	-3.76	-1,101	-12.51

6. REFERENCES

1. U.S. Department of Energy, National Solar Data Network, Prepared under Contract Number EG-77-C-01-4049, by IBM Corporation, December, 1977.

2. J. T. Smok, V. S. Sohoni, J. M. Nash, "Processing of Instrumented Data for the National Solar Heating and Cooling Demonstration Program," Conference on Performance Monitoring Techniques for Evaluation of Solar Heating and Cooling Systems, Washington, D.C., April, 1978.

3. E. Streed, et. al., Thermal Data Requirements and Performance Evaluation Procedures for the National Solar Heating and Cooling Demonstration Program, NBSIR 76-1137, National Bureau of Standards, Washington, August, 1976.

4. Mears, J. C. Reference Monthly Environmental Data for Systems in the National Solar Data Network. Department of Energy report SOLAR/0019-79/36. Washington, D.C., 1979.

5. ASHRAE Standard 93-77, Methods of Testing to Determine the Thermal Performance of Solar Collectors, The American Society of Heating, Refrigeration and Air Conditioning Engineers, Inc., New York, NY, 1977.

6. ASHRAE Standard 94-77, Methods of Testing Thermal Storage Devices Based on Thermal Performance, The American Society of Heating, Refrigeration and Air Conditioning Engineers, Inc., New York, NY, 1977.

7. D. J. Close and M. B. Yusoff, "The Effect of Air Leaks on Solar Collector Behaviour", Solar Energy, Vol. 22, pp 439-463 Pergamon Press 1978.

8.* Monthly Performance Report, Howard's Grove School, SOLAR/2041-78/09, Washington: Department of Energy, September 1978.

9.* Monthly Performance Report, Howard's Grove School, SOLAR/2041-78/10, Washington, Department of Energy, October 1978.

10.* Monthly Performance Report, Howard's Grove School, SOLAR/2041-78/11, Washington: Department of Energy, November 1978.

11.* Monthly Performance Report, Howard's Grove School, SOLAR/2041-78/12, Washington: Department of Energy, December 1978.

12.* Monthly Performance Report, Howard's Grove School, SOLAR/2041-79/01, Washington: Department of Energy, January 1979.

13.* Monthly Performance Report, Howard's Grove School, SOLAR/2041-79/02, Washington: Department of Energy, February 1979.

14.* Monthly Performance Report, Howard's Grove School, SOLAR/2041-79/03, Washington: Department of Energy, March 1979.

15.* Monthly Performance Report, Howard's Grove School, SOLAR/2041-79/04, Washington: Department of Energy, April 1979.

16. McCumber, W. H. Jr., "Collector Array Performance for Instrumented Sites of the National Solar Heating and Cooling Demonstration Program," to be published and distributed at the 1979 Solar Update Conference.

*Copies of these reports may be obtained from Technical Information Center, P. O. Box 62, Oak Ridge, Tennessee 37830.

APPENDIX A
DEFINITION OF PERFORMANCE FACTORS AND SOLAR TERMS

COLLECTOR ARRAY PERFORMANCE

The collector array performance is characterized by the amount of solar energy collected with respect to the energy available to be collected.

- INCIDENT SOLAR ENERGY (SEA) is the total insolation available on the gross collector array area. This is the area of the collector array energy-receiving aperture, including the framework which is an integral part of the collector structure.

- OPERATIONAL INCIDENT ENERGY (SEOP) is the amount of solar energy incident on the collector array during the time that the collector loop is active (attempting to collect energy).

- COLLECTED SOLAR ENERGY (SECA) is the thermal energy removed from the collector array by the energy transport medium.

- COLLECTOR ARRAY EFFICIENCY (CAREF) is the ratio of the energy collected to the total solar energy incident on the collector array. It should be emphasized that this efficiency factor is for the collector array, and available energy includes the energy incident on the array when the collector loop is inactive. This efficiency must not be confused with the more common collector efficiency figures which are determined from instantaneous test data obtained during steady state operation of a single collector unit. These efficiency figures are often provided by collector manufacturers or presented in technical journals to characterize the functional capability of a particular collector design. In general, the collector panel maximum efficiency factor will be significantly higher than the collector array efficiency reported here.

STORAGE PERFORMANCE

The storage performance is characterized by the relationships among the energy delivered to storage, removed from storage, and the subsequent change in the amount of stored energy.

- ENERGY TO STORAGE (STEI) is the amount of energy, both solar and auxiliary, delivered to the primary storage medium.

- ENERGY FROM STORAGE (STEO) is the amount of energy extracted by the load subsystems from the primary storage medium.

- CHANGE IN STORED ENERGY (STECH) is the difference in the estimated stored energy during the specified reporting period, as indicated by the relative temperature of the storage medium (either positive or negative value).

- STORAGE AVERAGE TEMPERATURE (TST) is the mass-weighted average temperature of the primary storage medium.

- STORAGE EFFICIENCY (STEFF) is the ratio of the sum of the energy removed from storage and the change in stored energy to the energy delivered to storage.

ENERGY COLLECTION AND STORAGE SUBSYSTEM

The Energy Collection and Storage Subsystem (ECSS) is composed of the collector array, the primary storage medium, the transport loops between these, and other components in the system design which are necessary to mechanize the collector and storage equipment.

- INCIDENT SOLAR ENERGY (SEA) is the total insolation available on the gross collector array area. This is the area of the collector array energy-receiving aperture, including the framework which is an integral part of the collector structure.

- AMBIENT TEMPERATURE (TA) is the average temperature of the outdoor environment at the site.

- ENERGY TO LOADS (SEL) is the total thermal energy transported from the ECSS to all load subsystems.

- AUXILIARY THERMAL ENERGY TO ECSS (CSAUX) is the total auxiliary supplied to the ECSS, including auxiliary energy added to the storage tank, heating devices on the collectors for freeze-protection, etc.

- ECSS OPERATING ENERGY (CSOPE) is the critical operating energy required to support the ECSS heat transfer loops.

SPACE HEATING SUBSYSTEM

The space heating subsystem is characterized by performance factors accounting for the complete energy flow to and from the subsystem. The average building temperature and the average ambient temperature are tabulated to indicate the relative performance of the subsystem in satisfying the space heating load and in controlling the temperature of the conditioned space.

- SPACE HEATING LOAD (HL) is the sensible energy added to the air in the building.

- SOLAR FRACTION OF LOAD (HSFR) is the fraction of the sensible energy added to the air in the building derived from the solar energy system.

- SOLAR ENERGY USED (HSE) is the amount of solar energy supplied to the space heating subsystem.

- OPERATING ENERGY (HOPE) is the amount of electrical energy required to support the subsystem, (e.g., fans, pumps, etc.) and which is not intended to affect directly the thermal state of the subsystem.

- AUXILIARY THERMAL USED (HAT) is the amount of energy supplied to the major components of the subsystem in the form of thermal energy in a heat transfer fluid or its equivalent. This term also includes the converted electrical and fossil fuel energy supplied to the subsystem.

- AUXILIARY ELECTRICAL FUEL (HAE) is the amount of electrical energy supplied directly to the subsystem.

- ELECTRICAL ENERGY SAVINGS (HSVE) is the estimated difference between the electrical energy requirements of an alternative conventional system (carrying the full load) and the actual electrical energy required by the subsystem.

- BUILDING TEMPERATURE (TB) is the average heated space dry bulb temperature.

- AMBIENT TEMPERATURE (TA) is the average ambient dry bulb temperature at the site.

ENVIRONMENTAL SUMMARY

The environmental summary is a collection of the weather data which is generally instrumented at each site in the program. It is tabulated in this data report for two purposes--as a measure of the conditions prevalent during the operation of the system at the site, and as an historical record of weather data for the vicinity of the site.

- TOTAL INSOLATION (SE) is accumulated total solar energy incident upon the gross collector array measured at the site.

- AMBIENT TEMPERATURE (TA) is the average temperature of the environment at the site.

- WIND DIRECTION (WDIR) is the average direction of the prevailing wind.

- WIND SPEED (WIND) is the average wind speed measured at the site.

- DAYTIME AMBIENT TEMPERATURE (TDA) is the temperature during the period from three hours before solar noon to three hours after solar noon.

APPENDIX B

SOLAR ENERGY SYSTEM PERFORMANCE EQUATIONS FOR THE NORTHVIEW SCHOOL, HOWARD'S GROVE, WISCONSIN

I. INTRODUCTION

Solar energy system performance is evaluated by performing energy balance calculations on the system and its major subsystems. These calculations are based on physical measurement data taken from each subsystem every 320 seconds. This data is then numerically combined to determine the hourly, daily, and monthly performance of the system. This appendix describes the general computational methods and the specific energy balance equations used for this evaluation.

Data samples from the system measurements are numerically integrated to provide discrete approximations of the continuous functions which characterize the system's dynamic behavior. This numerical integration is performed by summation of the product of the measured rate of the appropriate performance parameters and the sampling interval over the total time period of interest.

There are several general forms of numerical integration equations which are applied to each site. These general forms are exemplified as follows: The total solar energy available to the collector array is given by

$$\text{SOLAR ENERGY AVAILABLE} = (1/60)\ \Sigma\ [\text{IOOI} \times \text{AREA}] \times \Delta\tau$$

where IOOI is the solar radiation measurement provided by the pyranometer in Btu/ft^2-hr, AREA is the area of the collector array in square feet, $\Delta\tau$ is the sampling interval in minutes, and the factor (1/60) is included to correct the solar radiation "rate" to the proper units of time.

Similarly, the energy flow within a system is given typically by

$$\text{COLLECTED SOLAR ENERGY} = \Sigma\ [M100 \times \Delta H] \times \Delta\tau$$

where M100 is the mass flow rate of the heat transfer fluid in lb_m/min and ΔH is the enthalpy change, in Btu/lb_m, of the fluid as it passes through the heat exchanging component.

For a liquid system ΔH is generally given by

$$\Delta H = \overline{C}_p\ \Delta T$$

where $\overline{C}_p$ is the average specific heat, in Btu/(lb_m-°F), of the heat transfer fluid and ΔT, in °F, is the temperature differential across the heat exchanging component.

For an air system ΔH is generally given by

$$\Delta H = H_a(T_{out}) - H_a(T_{in})$$

where $H_a(T)$ is the enthalpy, in Btu/lb_m, of the transport air evaluated at the inlet and outlet temperatures of the heat exchanging component.

$H_a(T)$ can have various forms, depending on whether or not the humidity ratio of the transport air remains constant as it passes through the heat exchanging component.

For electrical power, a general example is

$$\text{ECSS OPERATING ENERGY} = (3413/60)\ \Sigma\ [EP100] \times \Delta\tau$$

where EP100 is the power required by electrical equipment in kilowatts and the two factors (1/60) and 3413 correct the data to Btu/min.

These equations are comparable to those specified in "Thermal Data Requirements and Performance Evaluation Procedures for the National

Solar Heating and Cooling Demonstration Program." This document, given in the list of references, was prepared by an inter-agency committee of the government, and presents guidelines for thermal performance evaluation.

Performance factors are computed for each hour of the day. Each numerical integration process, therefore, is performed over a period of one hour. Since long-term performance data is desired, it is necessary to build these hourly performance factors to daily values. This is accomplished, for energy parameters, by summing the 24 hourly values. For temperatures, the hourly values are averaged. Certain special factors, such as efficiencies, require appropriate handling to properly weight each hourly sample for the daily value computation. Similar procedures are required to convert daily values to monthly values.

EQUATIONS USED IN MONTHLY PERFORMANCE REPORT

NOTE: - MEASUREMENT NUMBERS REFERENCE SYSTEM SCHEMATIC FIGURE 3-1

SITE SUMMARY REPORT

INCIDENT SOLAR ENERGY (BTU)

$$SEA = (1/60) \sum [I001 \times AREA] \times \Delta\tau$$

INCIDENT SOLAR ENERGY PER UNIT AREA (BTU/SQ FT)

$$SE = (1/60) \sum I001 \times \Delta\tau$$

HUMIDITY RATIO FUNCTION (BTU/LBM)

$$HRF = 0.24 + 0.44 \times HR$$

WHERE 0.24 IS THE SPECIFIC HEAT AND HR IS THE HUMIDITY RATIO OF THE TRANSPORT AIR. THIS FUNCTION IS USED WHENEVER THE HUMIDITY RATIO WILL REMAIN CONSTANT AS THE TRANSPORT AIR FLOWS THROUGH A HEAT EXCHANGING DEVICE.

COLLECTED SOLAR ENERGY (BTU)

$$SECA = \sum [M100 \times HRF \times (T150 - T100)] \times \Delta\tau$$

COLLECTED SOLAR ENERGY PER UNIT AREA (BTU/SQ FT)

$$SEC = \sum [M100 \times HRF \times (T150 - T100)/AREA] \times \Delta\tau$$

AVERAGE AMBIENT TEMPERATURE (°F)

$$TA = (1/60) \sum T001 \times \Delta\tau$$

AVERAGE BUILDING TEMPERATURE (°F)

$$TB = (1/60) \sum T600 \times \Delta\tau$$

ECSS SOLAR CONVERSION EFFICIENCY

CSCEF = SOLAR ENERGY TO LOAD/INCIDENT SOLAR ENERGY

ECSS OPERATING ENERGY (BTU)

$$CSOPE = 56.8833 \times \sum EP101 \times \Delta\tau$$

TOTAL SYSTEM OPERATING ENERGY (BTU)

SYSOPE = ECSS OPERATING ENERGY + HEATING OPERATING ENERGY

TOTAL ENERGY CONSUMED (BTU)

TECSM = AUXILIARY ENERGY + SYSTEM OPERATING ENERGY + SOLAR ENERGY COLLECTED

LOAD SUBSYSTEM SUMMARY (BTU)

HL= HEATING SOLAR ENERGY + HEATING AUXILIARY THERMAL ENERGY

HEATING AUXILIARY FOSSIL FUEL (BTU)

HAF = HF x EP406/BOILPWR x FUELFL

WHERE HF IS THE HEAT CONTENT OF THE FOSSIL FUEL

WHERE BOILPWR IS MAGNITUDE OF FUEL OIL PUMP POWER ON FOR ONE FULL SCAN

WHERE FUELFL IS BOILER FUEL FLOW RATE

TOTAL AUXILIARY FOSSIL FUEL (BTU)

AXF = HEATING AUXILIARY FOSSIL FUEL

HEATING ELECTRICAL SAVINGS (BTU)

$$HSVE = \Sigma \left[56.8833 \times \left(EP406 + EP403 + EP402 \times \frac{\text{HEATING AUXILIARY THERMAL ENERGY}}{\text{HEATING LOAD}}\right) \times \frac{\text{HEATING LOAD}}{\text{HEATING AUXILIARY THERMAL ENERGY}}\right] - \text{HEATING OPERATING ENERGY}$$

TOTAL ELECTRICAL SAVINGS (BTU)

TSVE = HEATING ELECTRICAL SAVINGS

HEATING FOSSIL SAVINGS (BTU)

HSVF = (HEATING SOLAR ENERGY/HEFF)

WHERE HEFF IS THE AUXILIARY CONVERSION EFFICIENCY

SYSTEM LOAD (BTU)

SYSL = HEATING LOAD

HEATING SOLAR FRACTION (PERCENT)

HSFR = 100 x (HEATING SOLAR ENERGY/HEATING LOAD)

SYSTEM SOLAR FRACTION (PERCENT)

SFR = HEATING LOAD x HEATING SOLAR FRACTION)/SYSTEM LOAD x 100

HEATING SOLAR ENERGY (BTU)

HSE = Σ (M001 + M400 + M403 - M402) x (T450 - TINBED) x HRF x $\Delta\tau$

WHENEVER IN HEATING MODE

WHERE TINBED IS AVERAGE OF LOWER ROCK BED TEMPERATURES

TOTAL SOLAR ENERGY TO LOADS (BTU)

SEL = HEATING SOLAR ENERGY

OPERATING ENERGY (BTU):

HEATING OPERATING ENERGY

HOPE = Σ [56.88 x (EP402 + EP403 + EP406)] x $\Delta\tau$

HEATING AUXILIARY THERMAL ENERGY (BTU)

HAT = HF x HEFF * EP406/BOILPWR * FUELFL

WHERE HF IS THE HEAT CONTENT OF THE FOSSIL FUEL AND HEFF IS THE CONVERSION EFFICIENCY

WHERE BOILPWR IS MAGNITUDE OF FUEL OIL PUMP ON FOR ONE FULL SCAN

WHERE FUELFL IS BOILER FUEL FLOW RATE

TOTAL AUXILIARY THERMAL ENERGY (BTU)

AXT = HEATING AUXILIARY THERMAL ENERGY

TOTAL FOSSIL SAVINGS (BTU)

TSVF = HEATING FOSSIL SAVINGS

SYSTEM PERFORMANCE FACTOR

SYSPF = SYSTEM LOAD/[(AUXILIARY FOSSIL FUEL + 3.33 x (AUXILIARY ELECTRIC FUEL + SYSTEM OPERATING ENERGY)]

OPERATIONAL INCIDENT ENERGY (BTU)

SEOP = 1/60 Σ [I001 x AREA] x $\Delta\tau$

COLLECTOR ARRAY EFFICIENCY

CAREF = SOLAR ENERGY COLLECTED/INCIDENT SOLAR ENERGY

ENERGY TO STORAGE (BTU)

$$STEI = \Sigma [M100 \times (T150 - T100) \times HRF] \times \Delta\tau$$

ENERGY FROM STORAGE (BTU)

$$STEO = \Sigma (M001 + M400 + M403 - M402) \times (T450 - TINBED) \times HRF \times \Delta\tau$$

WHERE TINBED IS AVERAGE OF LOWER ROCK BED TEMPERATURES

CHANGE IN STORED ENERGY (BTU)

STECH = STORAGE CAPACITY x [HEAT CONTENT PREVIOUS SCAN - HEAT CONTENT PRESENT SCAN] x [1 - VOID FRACTION]

WHERE STORAGE CAPACITY IS THE ACTIVE VOLUME IN TANK AND VOID FRACTION IS RATIO OF VOLUME OF AIR TO VOLUME OF ROCK

STORAGE AVERAGE TEMP (°F)

$$TST = 1/60 \Sigma [(T201 + T202 + T203 + T204 + T205 + T206 + T207 + T208 + T209 + T210 + T212) / 12] \times \Delta\tau$$

STORAGE EFFICIENCY

STEFF = (CHANGE IN STORED ENERGY + ENERGY FROM STORAGE) / ENERGY TO STORAGE

DAYTIME AMBIENT TEMP (°F)

$$TDA = (1/360) \Sigma [T001] \times \Delta\tau$$

$\pm$ 3 HOURS FROM SOLAR NOON

WIND DIRECTION (DEGREES)

$$WDIR = (1/60) \Sigma [D001] \times \Delta\tau$$

WIND SPEED (M.P.H.)

$$WIND = (1/60) \Sigma [V001] \times \Delta\tau$$

APPENDIX C

LONG-TERM AVERAGE WEATHER CONDITIONS

SITE: HOWARDS GROVE 154. LOCATION: HOWRDS GROVE WI

ANALYST: K. SHENFISH FDRIVE NO.: 60.

COLLECTOR TILT: 50.00 (DEGREES) COLLECTOR AZIMUTH: 0.0 (DEGREES)

LATITUDE: 43.13 (DEGREES) RUN DATE: 6/04/79

MONTH	HOBAR	HBAR	KBAR	RBAR	SBAR	HDD	CDD	TBAR
JAN	1158.	465.	0.40106	1.852	860.	1476	0	17.
FEB	1633.	730.	0.44700	1.552	1133.	1253	0	20.
MAR	2264.	1095.	0.48362	1.250	1368.	1085	0	30.
APR	2942.	1442.	0.49003	0.999	1440.	623	0	44.
MAY	3436.	1744.	0.50756	0.857	1494.	343	13	54.
JUN	3643.	1943.	0.53337	0.799	1553.	91	76	65.
JUL	3536.	1925.	0.54435	0.824	1585.	19	160	70.
AUG	3130.	1670.	0.53363	0.937	1565.	45	152	69.
SEP	2506.	1265.	0.50459	1.145	1448.	166	16	60.
OCT	1816.	863.	0.47505	1.458	1258.	465	3	50.
NOV	1268.	494.	0.38957	1.724	852.	891	0	35.
DEC	1031.	365.	0.35391	1.866	681.	1316	0	23.

LEGEND:

HOBAR ==> MONTHLY AVERAGE DAILY EXTRATERRESTRIAL RADIATION (IDEAL) IN BTU/DAY-FT2.

HBAR ==> MONTHLY AVERAGE DAILY RADIATION (ACTUAL) IN BTU/DAY-FT2.

KBAR ==> RATIO OF HBAR TO HOBAR.

RBAR ==> RATIO OF MONTHLY AVERAGE DAILY RADIATION ON TILTED SURFACE TO THAT ON A HORIZONTAL SURFACE FOR EACH MONTH (I.E., MULTIPLIER OBTAINED BY TILTING).

SBAR ==> MONTHLY AVERAGE DAILY RADIATION ON A TILTED SURFACE (I.E., RBAR * HBAR) IN BTU/DAY-FT2.

HDD ==> NUMBER OF HEATING DEGREE DAYS PER MONTH.

CDD ==> NUMBER OF COOLING DEGREE DAYS PER MONTH.

TBAR ==> AVERAGE AMBIENT TEMPERATURE IN DEGREES FAHRENHEIT.